Cell Research (2009) 19:1205-1216.

www.nature.com/cr

ORIGINAL ARTICLE

A novel chloroplast-localized protein EMB1303 is required for chloroplast development in *Arabidopsis*

Xiaozhen Huang[1], Xiaoyan Zhang[1], Shuhua Yang[1, 2]

[1]*State Key Laboratory of Plant Physiology and Biochemistry, College of Biological Sciences, China Agricultural University, Beijing 100193, China;* [2]*National Plant Gene Research Center, Beijing 100193, China*

To understand the molecular mechanisms underlying chloroplast development, we isolated and characterized the albino mutant *emb1303-1* in *Arabidopsis*. The mutant displayed a severe dwarf phenotype with small albino rosette leaves and short roots on a synthetic medium containing sucrose. It is pigment-deficient and seedling lethal when grown in soil. Embryo development was delayed in the mutant, although seed germination was not significantly impaired. The plastids of *emb1303-1* were arrested in early developmental stages without the classical stack of thylakoid membrane. Genetic and molecular analyses uncovered that the *EMB1303* gene encodes a novel chloroplast-localized protein. Microarray and RT-PCR analyses revealed that a number of nuclear- and plastid-encoded genes involved in photosynthesis and chloroplast biogenesis were substantially downregulated in the mutant. Moreover, the accumulation of several major chloroplast proteins was severely compromised in *emb1303-1*. These results suggest that EMB1303 is essential for chloroplast development.

***Keywords*:** EMB1303, albino, chloroplast development, embryogenesis, *Arabidopsis*

Cell Research (2009) **19**:1205-1216. doi: 10.1038/cr.2009.84; published online 7 July 2009

Introduction

Chloroplast is a special and important organelle of plant cells carrying out many essential processes such as photosynthesis and biosynthesis of fatty acids, pigments, and amino acids from inorganic nitrogen [1].

In addition to the outer and inner membrane, mature chloroplasts have an internal membrane network of thylakoids, where the light reactions take place, converting the light energy into chemical energy stored in ATP and NADPH. The formation of the chloroplast complex and elaborate thylakoid membrane initiates from proplastids and is dependent on the coordinated expression of nuclear- and plastid-encoded genes [2, 3]. These genes encode proteins involved in many processes of chloroplast development such as RNA processing, protein translation and folding, and protein transport. Such proteins include PAC, a nuclear-encoded protein functioning in plastid mRNA maturation and accumulation [4]; HCF136, a chaperone-like assembly factor for the stability of photosystem II (PSII) [5]; SLP, chaperonin-60α for protein folding [6]; APG2, a major component of ΔpH-dependent thylakoid protein transporter [7]; and ALB3, a subunit of the thylakoid Sec protein transport system [8, 9]. Loss of these proteins usually impairs chloroplast development resulting in abnormal chloroplast morphology. Chloroplast is also involved in the biosynthesis of plastid isoprenoids such as chlorophyll and carotenoid. Mutations in the isoprenoid biosynthesis pathways, such as *cla1*, *ispD*, *ispE*, *ispG*, *ispH*, *pds3*, and *zds*, block chloroplast development and result in albino phenotype [10-14].

Chloroplast development is tightly linked to embryogenesis. Mutants interfering with or blocking chloroplast development usually exhibit embryogenesis defects [6, 15-19]. For example, mutations in some genes participating in chloroplast membrane lipid biosynthesis result in embryonic lethality [20, 21]. However, a deficiency in the photosynthetic capacity of embryo plastids does not always cause an embryonic lethal phenotype. Some albino and pigment-deficient mutants produce morphologically normal seeds that are able to germinate and grow to

Correspondence: Shuhua Yang
Tel: +86-10-62734838; Fax: +86-10-62734838
E-mail: yangshuhua@cau.edu.cn
Received 1 March 2009; revised 20 March 2009; accepted 14 April 2009; published online 7 July 2009

variable extent in the presence of sugar [22]. Similarly, the majority of mutations in genes involved in photosynthesis, such as *VAR2*, *PsbP*, and *CHL27*, do not confer embryonic lethality, but produce pale green to yellow or variegated seedlings [1, 23, 24]. Mutations in genes in plastid isoprenoid biosynthesis pathways, such as *CLA1*, *PDS3*, and *ZDS*, do not show embryonic lethal phenotype either [10, 13, 14].

Despite the discovery of many genes involved in chloroplast development, we still do not have a full understanding of the complex biogenesis of this organelle. In this study, we isolated an albino mutant *emb1303-1*, which is defective in a gene coding for a new chloroplast protein. Physiological and molecular analyses suggest that EMB1303 plays an essential role in both chloroplast development and plant growth.

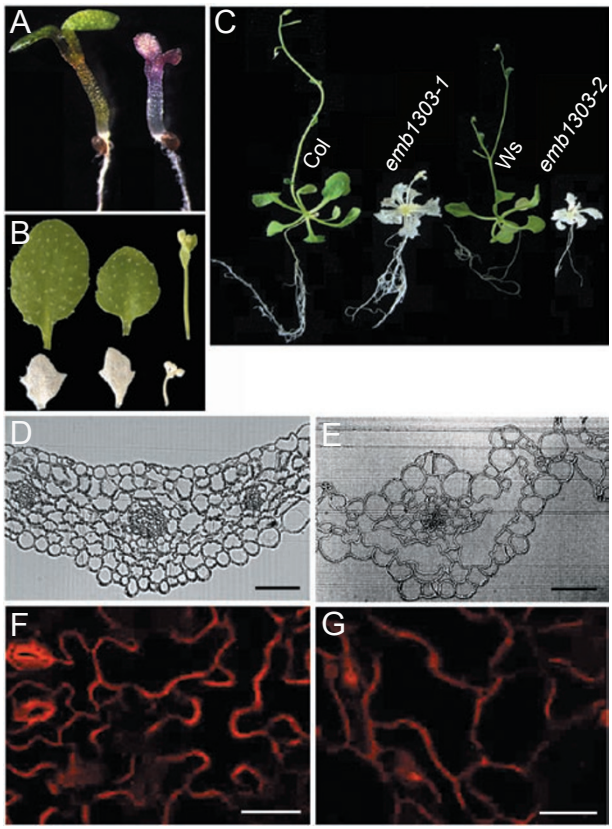

Figure 1 Growth phenotypes of the *emb1303* mutants. Wild-type and the *emb1303* mutant seeds were grown at 22 ºC under long-light conditions for 5 days **(A)**, and 35 days **(C)**. **(B)** Leaves and inflorescences of wild type (top) and *emb1303-1* (bottom). **(D**, **E)** Cross-sections of leaves from the wild type **(D)** and *emb1303-1* **(E)**. Bar: 100 μm. **(F**, **G)** Pavement cells from true leaves of wild type **(F)** and *emb1303-1* **(G)** stained by propidium iodide. Bar: 100 μm.

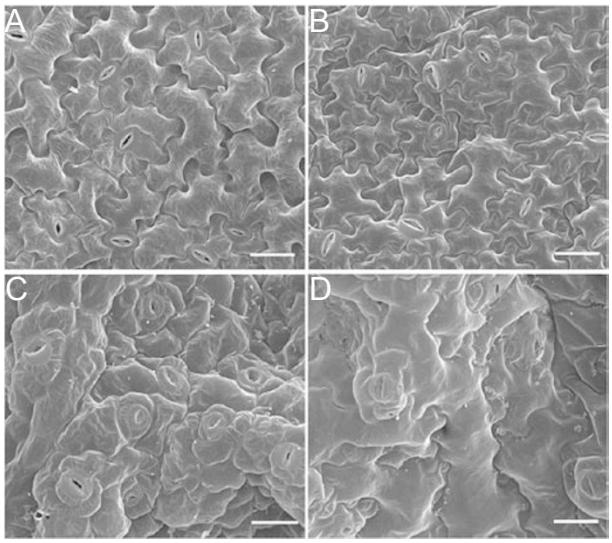

Figure 2 Scanning electron microscope images of leaf epidermis of the *emb1303* mutant. Adaxial **(A**, **C)**, and abaxial **(B**, **D)** leaves from wild-type Col and *emb1303-1* mutant are shown. Plants were grown on 1/2 MS medium supplemented with 2% sucrose for 14 days and the second leaves are shown. Bar: 100 μm.

Results

Isolation and phenotypic characterization of an albino mutant

The albino mutant was isolated by screening *Arabidopsis* T-DNA insertion lines that had been mutagenized by T-DNA insertion (ABRC (Arabidopsis Biological Resource Center)). The homozygous mutant plants showed albino phenotype and died shortly after germination in soil. On Murashige-Skoog (MS) medium supplemented with 2% sucrose, the mutant plants germinated normally and had purple cotyledons that became white several days later (Figure 1A). The growth of the mutant was arrested in subsequent development with smaller rosette leaves and shorter roots compared to the Col-0 wild type (Figure 1B and 1C). The mutant had swollen white leaves with curved and abnormal edges. Light microscopy analysis showed that the mutant leaves had a reduced number of mesophyll cells with large intercellular spaces and lacked defined mesophyll layers (Figure 1D and 1E). The pavement cells in the mutant leaf epidermis did not have the interlocking jigsaw puzzle-shape but were rather rectangular or spindle-like (Figure 1F and 1G). Scanning electron microscopy analysis showed that pavement cells at both abaxial and adaxial surfaces were abnormal in the mutant, and the lobes of the cell were dramatically eliminated compared to the wild type (Figure 2).

The primary root of the mutant was much shorter than

that of the wild type (Figure 1C). When grown on the medium containing norflurazon that blocks the synthesis of chlorophyll and carotenoid, the mutant still had shorter primary root compared to the wild type (data not shown). This suggests that the impaired root development is partially independent of the chlorophyll and carotenoid levels. The mutant could bolt eventually in tissue culture with sucrose, but the flowers were infertile.

Molecular characterization and complementation of emb1303

To investigate the nature of the mutation, we analyzed the progeny of a backcross between the mutant and the wild-type Col-0. All of the F1 progeny (n = 18) showed a normal phenotype, indicating that the mutation was recessive. Among the 350 F2 progeny, the mutant phenotype segregated at a 1:3 ratio (mutant:WT = 88:270, χ^2 = 0.059, $P < 0.05$). Further analysis showed that all the 88 albino plants were kanamycin-resistant (Kan-R). We also randomly chose 200 Kan-R individuals from the F2 and found that the albino phenotype segregated at a 1:2 ratio (mutant:WT = 64:136, χ^2 = 0.202, $P < 0.05$). These results suggest that the albino phenotype is tightly linked to a T-DNA insertion at a single locus.

The flanking sequences of the T-DNA insertion were amplified by thermal asymmetric interlaced PCR. Two left borders of the T-DNA insertion were found to be located in the upstream and downstream of *At1g56200* (Figure 3A). Further PCR analysis revealed that the genomic fragment of *At1g56200* was deleted in the mutant. *At1g56200* was previously annotated as *Embryo Defective 1303* (*EMB1303*), and we therefore named this mutant as *emb1303-1* hereafter.

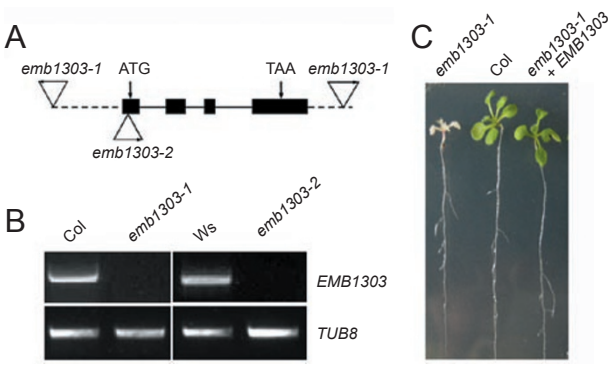

Figure 3 Isolation of the *emb1303* mutants. **(A)** A schematic diagram of genomic structure of the *EMB1303* gene. Filled boxes and lines indicate exons and introns, respectively. Positions of T-DNA insertions are indicated by triangles with left border indicated by arrows. The T-DNA insertion site in *emb1303-1* spans *EMB1303* gene, leading to a deletion of the gene. The T-DNA in *emb1303-2* is located at 5′-UTR of *EMB1303*. **(B)** RT-PCR analysis of *EMB1303* transcripts in the wild type and *emb1303* mutants. *β-tubulin* gene *TUB8* was used as a control. **(C)** Complementation of the *emb1303-1* mutant with genomic fragment of *EMB1303* gene.

To confirm that the disruption of *EMB1303* is responsible for the albino phenotype, we cloned a 5.2-kb wild-type genomic fragment of *EMB1303* from the BAC clone F14G9, and transformed it into heterozygous *emb1303-1* plants. Among 48 T1 transgenic lines analyzed, 13 lines were homozygous *emb1303-1* and they showed a wild-type looking phenotype (Figure 3C). We also identified a second mutant allele *emb1303-2* (CS16150) in Ws background from ABRC. *emb1303-2* carried a T-DNA insertion at 5′-UTR of *At1g56200* (Figure 3A), and exhibited a similar phenotype to *emb1303-1* (Figure 1C). RT-PCR analysis showed that the T-DNA insertions abolished *EMB1303* mRNA expression in both alleles of *emb1303* (Figure 3B), indicating that they are loss-of-function mutants. Collectively, these results demonstrate that *EMB1303* is indeed *At1g56200*. Since these two alleles showed similar phenotypes, we chose *emb1303-1* for further studies unless specified otherwise.

Molecular characterization of EMB1303

There are two splicing variants of *EMB1303* cDNA with four exons and three introns each in *Arabidopsis*, thus encoding two putative proteins with 151 and 154 amino acids, respectively. A BLAST search revealed that the predicted EMB1303 protein and its homolog (At1g30475) in *Arabidopsis* share 57% identity and 71% similarity at the amino acid level (Supplementary information, Figure S1). EMB1303 also shares significant identity with the rice proteins LOC_Os02g17380, LOC_Os02g05890, LOC_Os06g22660, *Megicago truncatula* protein ACJ85874, and rape protein CAO45180, with high degrees of conservation at the carboxyl-terminus. However, these proteins do not have known domains or motifs predicted by any available bioinformatics tools, and no functional data are available in plants.

In order to elucidate the physiological function of EMB1303, we examined its organ-specific expression in *Arabidopsis*. *EMB1303* was strongly expressed in young leaves, roots, and flowers (Figure 4A). This result was validated by β-glucuronidase (GUS) staining on transgenic plants expressing GUS driven by the *EMB1303* promoter. The GUS activity was high in cotyledons and young rosette leaves, but low in stems (Figure 4B-4E). GUS expression was also detected in the open anthers, style and ovary walls, and young siliques, whereas it was not detected in young flower buds, immature pollen, or mature siliques (Figure 4F-4H). These results suggest

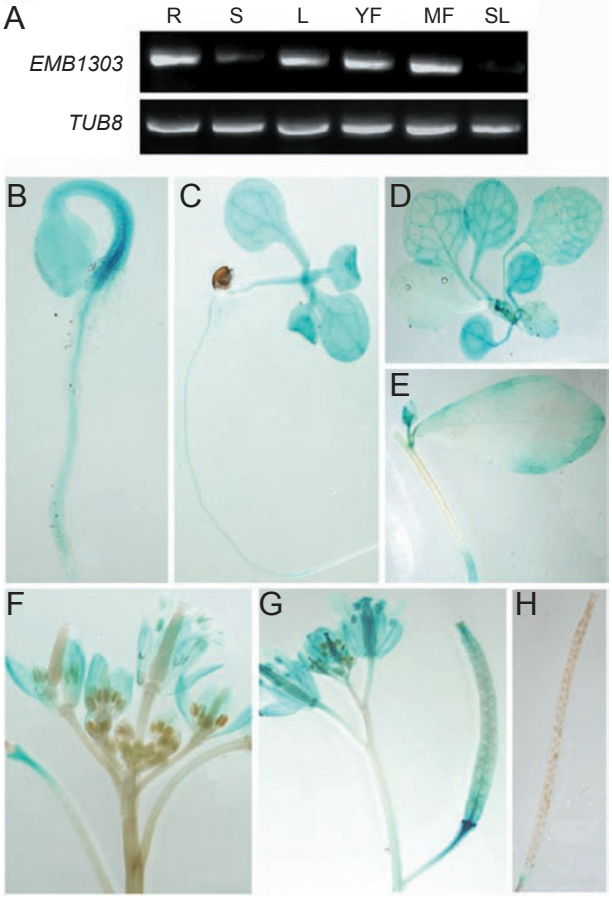

Figure 4 Spacial expression pattern of the *EMB1303* gene. **(A)** RT-PCR analysis of *EMB1303* transcripts in various organs of *Arabidopsis* plants. Total RNA was isolated from the following tissues: roots (R), stems (S), leaves (L), young flowers (YF), maturing flowers (MF), and mature siliques (SL) of Col plants grown under long-day conditions. RT-PCR was performed with *EMB1303*-specific primers (top gel) and *TUB8*-specific primers (bottom gel). **(B**-**H)** GUS expression in seedlings at the cotyledon **(B)**, four-leaf **(C)** and eight-leaf **(D)** stages, stem and cauline leaf **(E)**, inflorescence and flowers **(F**, **G)**, and mature silique **(H)** of *pEMB1303::GUS* transgenic plants.

that EMB1303 may function in a number of developmental stages.

We further generated transgenic plants overexpressing *EMB1303* under the control of CaMV 35S promoter. However, none of the transgenic plants showed visible growth defect phenotypes (data not shown), indicating that constitutive expression of *EMB1303* does not significantly affect growth and development.

Localization of the EMB1303 protein

P-Sort and Target P analyses predict that EMB1303 is likely targeted to the chloroplast. Computational transit peptide prediction [25] also reveals the presence of a probable chloroplast-targeting sequence at the N-terminal region of EMB1303.

To determine the subcellular localization of EMB1303, we generated a construct *p35S::EMB1303-GFP* containing genomic fragment of *EMB1303* fused in-frame to a synthetic green fluorescent protein at the C-terminal region. Transient expression of this fusion protein in *Arabidopsis* protoplasts and *Nicotiana benthamiana* leaves was examined by confocal microscopy. The green fluorescence was co-localized with the red autofluorescence of chlorophyll in leaf mesophyll cells of *N. benthamiana* (Figure 5A). The control protein expressed from *p35S::GFP* was localized ubiquitously. Further analysis showed that GFP signals were in the chloroplasts of the protoplasts isolated from leaves from *N. benthamiana* harboring *p35S::EMB1303-GFP* (Figure 5B). After these protoplasts were broken, the GFP fluorescence was still co-localized with the chloroplasts from *p35S::EMB1303-GFP* protoplasts, while the GFP signal was nearly abolished with the removal of the cytoplasm of *p35S::GFP* protoplasts, indicating that EMB1303-GFP is targeted to the chloroplast (Figure 5C). Similar results were obtained with transiently expressed *p35S::EMB1303-GFP* in *Arabidopsis* protoplasts (data not shown).

In addition, chloroplasts were isolated from protoplasts of *N. benthamiana* leaves harboring *p35S::EMB1303-GFP*, and the total proteins were subject to immunoblot analysis with an antibody against GFP protein. EMB1303-GFP protein was detected in chloroplast fraction with a molecular weight at approximately 37 kDa, which is smaller than the predicted molecular mass of 43 kDa for the full-length protein (Figure 5D). It is however consistent with the mass of the protein where the N-terminal signal sequence is removed after importing into the chloroplast. Taken together, these results indicate that EMB1303 is localized in the chloroplast.

Seedling morphology of emb1303-1

It is known that under relatively high light conditions, photo-oxidative stress occurs in the mutants defective in carotenoid biosynthesis, resulting in abnormal chloroplast development [26]. To determine whether the *emb1303-1* phenotype is caused by photo-oxidative stress or merely due to abnormal plastid development, we grew *emb1303-1* under different light conditions. Under high light, the growth of *emb1303-1* seedlings was arrested. A typical 14-day-old wild-type seedling had four true leaves and long primary root with multiple lateral shoots, whereas *emb1303-1* had only two small true leaves and one short primary root (Supplementary information, Figure S2A). The mutant showed slightly better growth

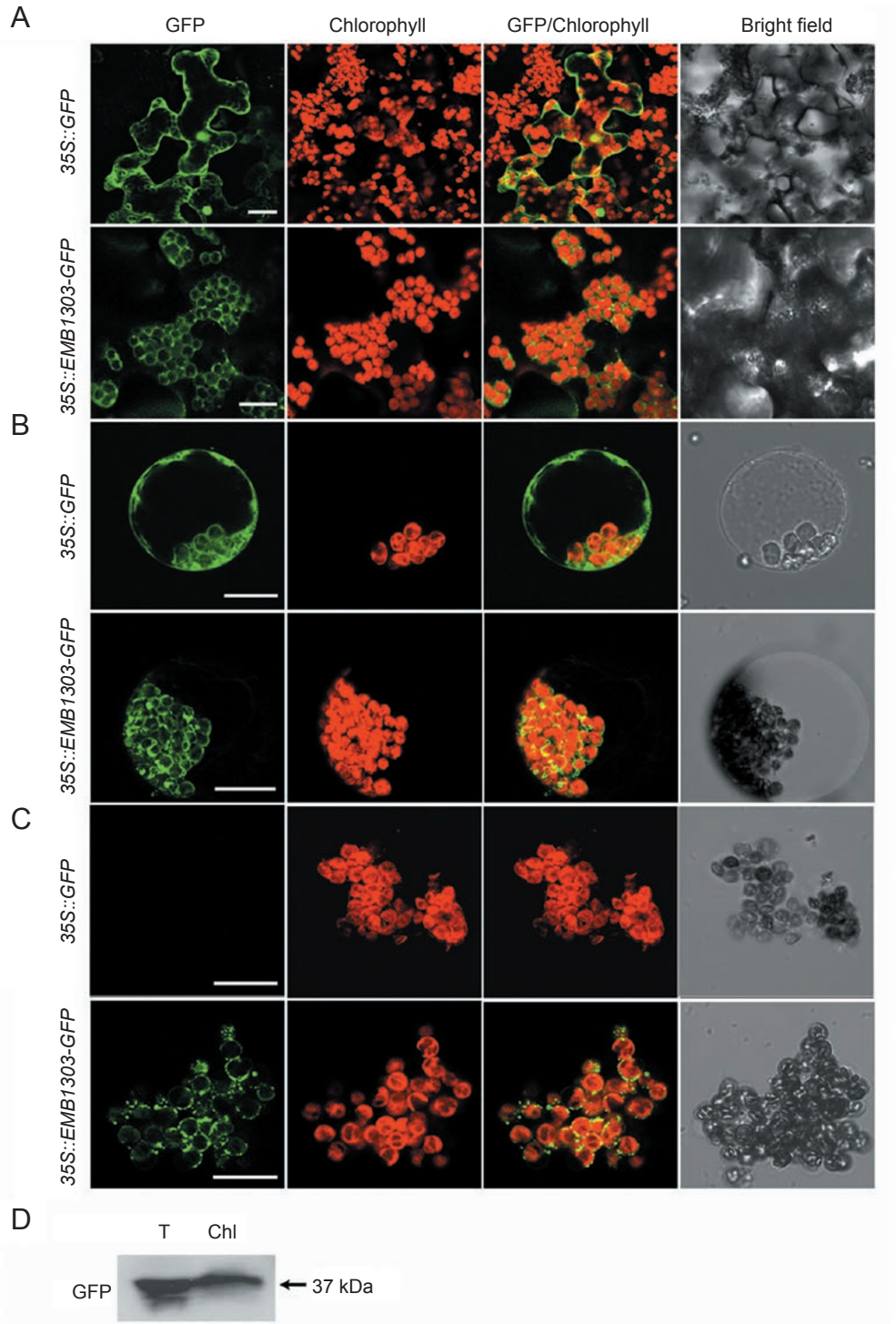

Figure 5 Subcellular localization of the EMB1303 protein in *N. bethamiana* leaves. *p35S::EMB1303-GFP* and *p35S::GFP* were transformed into *N. benthamiana* by *A. tumefaciens*-mediated infiltration. Signals were detected by a laser confocal-scanning microscope from intact leaf mesophyll cells **(A)**. **(B)** Protoplasts prepared from the same leaves as in **(A)** , and **(C)** broken protoplasts from **(B)**. Green fluorescence signals, chlorophyll red autofluorescence, an overlay of green and red signals, and bright-field images are shown in panels (in the order from left to right). Bar: 20 μm. **(D)** Immunoblot assay of proteins. Total proteins (T) and chloroplast proteins (Chl) were extracted from protoplasts prepared from the same leaves of **(A)** and analyzed by immunoblotting with polyclonal antibodies raised against GFP.

under low light or darkness than under high light, but the albino phenotype could not be rescued (Supplementary information, Figure S2B-2D). This result indicates that the albino phenotype of *emb1303-1* largely results from a block in plastid development, but not from the photo-oxidative damage caused by deficiency in photo-protective carotenoids.

It has been reported that glucose and sucrose regulate expression of genes involved in accumulation, mobilization, and storage of photosynthetic products [27], thus modulating plant growth and development. To investigate the effect of sugar on the growth of *emb1303-1*, we grew *emb1303-1* on MS media with or without sucrose. The development of *emb1303-1* was completely arrested after germination under sucrose-depleted condition, resembling growth in soil (Supplementary information, Figure S2E). In contrast, *emb1303-1* showed better growth on sucrose-containing medium (Figure 1B, Supplementary information, Figure S2F-2G). Besides, *emb1303-1* seedlings accumulated more anthocyanin under high sugar conditions than the wild type (data not shown), presumably due to the osmotic stress caused by sugar. These results demonstrate that the mutant is not able to grow photoautotrophically.

Embryogenesis in emb1303-1

A previous study reported that chloroplasts are formed transiently and transformed into storage organelles during early embryo development [28]. Since *emb1303-1* showed the albino phenotype, we speculate that embryogenesis in self-fertilizing heterozygous *emb1303-1* might be abnormal due to defective chloroplasts in the embryo. Within the immature siliques of the self-fertilizing heterozygous *emb1303-1*, abnormal white seeds were detected at a frequency of about 25% (Figure 6B, 6C) at early stages of embryogenesis. However, the seed color was indistinguishable between the wild type and the mutant after seed desiccation (Figure 6D), indicating a normal development of seed coat in *emb1303-1*.

Embryo development was further examined by Nomarski microscopy (Figure 6E-6N). It was difficult to distinguish the mutant seeds from the wild-type ones in the heterozygous siliques before the embryos became green. At the greening stage, albino white seeds were observed at a frequency of approximately 25% (white seeds:green seeds = 68:200). Moreover, development of the albino homozygous embryos was retarded. While the embryos of wild-type or heterozygous seeds (n = 158) have already developed into heart-shaped embryos (Figure 6E, 6G), the *emb1303-1* embryos (n = 54, equivalent to 25% of the total number 212) were still at the globular stage (Figure 6F, 6H). As green embryos of wild-type or heterozygous seeds (n = 151) progressed to the torpedo or early cotyledon stage (Figure 6I, 6K), embryo devel-

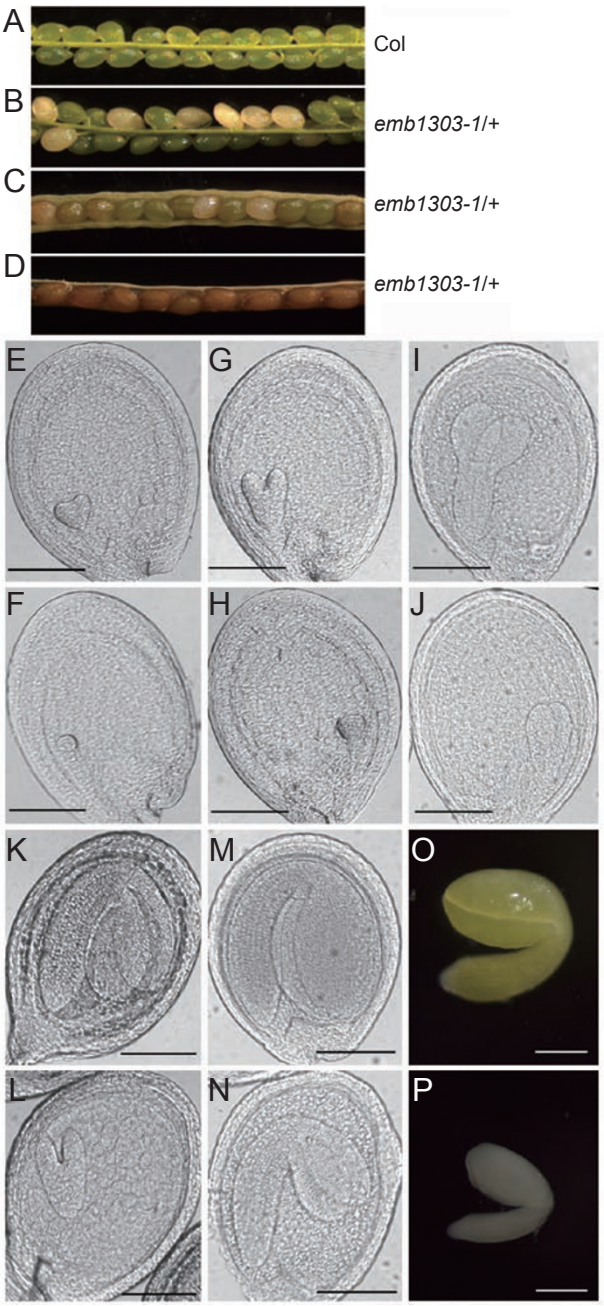

Figure 6 Phenotypes of *emb1303-1* embryos during seed development. **(A)** Wild-type seeds. **(B-D)** Seed segregation in siliques from an *emb1301*/+ heterozygous plant at different stages. Approximately, one-quarter of albino embryos segregated at early stages. **(E-P)** Cleared seeds observed under Nomarski optics. Embryo development of wild type **(E**, **G**, **I**, **K**, **M**, **O)** and *emb1303-1* **(F**, **H**, **J**, **L**, **N**, **P)** at globular, heart, torpedo and early cotyledon, and mature cotyledon stages. Bar: 100 μm.

opment of the homozygous seeds (n = 53) was delayed at the heart stage (Figure 6J, 6L). Nevertheless, tissue organization of the *emb1303-1* embryo appeared to be normal at early stages of embryogenesis. The homozygous seeds could form mature embryos eventually, although the size of embryos was small and the color was pale (Figure 6M-6P). These results demonstrate that embryo development of *emb1303-1* is delayed during early stages of seed development.

Content of chlorophyll and carotenoid in emb1303-1

It has been shown that many mutants in the methylerythritol 4-phosphate pathway, such as *cla1*, *clb4* (*ispG*), and *clb6* (*ispH*) in the non-cell-autonomous pathway, contain very low chlorophyll in the seedling, whereas their embryos accumulate significant levels of chlorophyll [29]. We examined autofluorescence in the embryos, and found that autofluorescence was much lower in *emb1303-1* than in the wild type (Supplementary information, Figure S3A-3B), indicating that *EMB1303* acts in a cell-autonomous manner.

We also measured the levels of pigments including chlorophyll and carotenoid in *emb1303-1* seedlings. The levels of chlorophyll and carotenoid in *emb1303-1* were approximately 1% and 5.7% of those of the wild type, respectively (Table 1). Consistent with this result, the chlorophyll autofluorescence of *emb1303-1* was much weaker than that of the wild type (Supplementary information, Figure S3C-3D).

Plastid development in emb1303-1

Loss of photosynthetic pigments may affect chloroplast development. To assess the effect of *EMB1303* mutation on chloroplast development, plastids from 28-day-seedling mesophyll cells were examined by transmission electron microscopy. In wild-type plants grown under normal light, chloroplasts were crescent-shaped and contained well-developed thylakoid membranes consisting of stroma thylakoids and grana thylakoids (Figure 7A, 7C). In contrast, plastids in *emb1303-1* could not develop into normal mature chloroplasts with the thylakoid membrane system. Instead, all mutant plastids were small, and lacked the lens-like structure typically observed in mature chloroplasts in the wild type (Figure 7B, 7D and 7E). The internal membranes were non-stacked and could not be differentiated into grana and stroma thylakoids. These results suggest that *EMB1303* may function in plastid differentiation via mediating internal thylakoid membrane formation. As the morphology of other organelles, such as the endoplasmic reticulum and mitochondria, was similar in the mutant and the wild type (Figure 7C and 7E), *EMB1303* mutation may specifically affect chloroplast biogenesis in leaves.

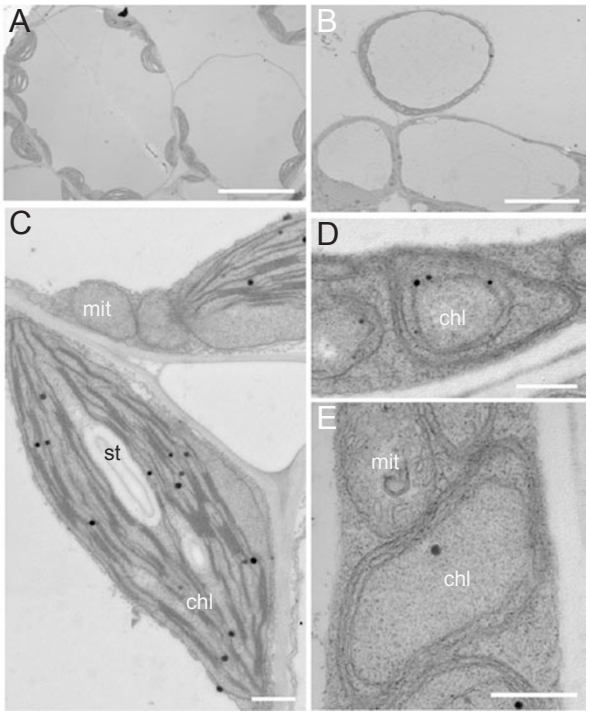

Figure 7 Transmission electron microscopy of plastids from *emb1301-1* seedlings. Plants were grown on 1/2 MS medium supplemented with 2% sucrose for 14 days and the second leaf of a representative plant for each phenotype category was fixed for transmission electron microscope analysis. **(A**, **B)** An overview of parenchyma cells. Bar: 10 μm. **(C**, **D**, **E)** Enlarged views of chloroplasts. Bar: 500 nm. chl, chloroplast; mit, mitochondrion; st, starch granule.

Table 1 Chlorophyll and carotenoid content of wild-type and *emb1303* seedlings

Genotype	Chlorophyll A	Chlorophyll B	Total chlorophyll	Total carotenoids
Wild type	433 ± 22.89	176 ± 20.98	609 ± 43.87	42 ± 4.50
emb1303-1	4.03 ± 0.46	2.81 ± 0.21	6.84 ± 0.68	2.41 ± 0.48

Pigments were extracted from 21-day-old seedlings and quantified by the method previously described [37]. Values given are $\mu g \cdot g^{-1}$ fresh weight ± SD. The average of three replicates is shown.

Expression of genes involved in chlorophyll biosynthesis and chloroplast development in emb1303-1

To elucidate possible effects of the *emb1303* mutation on the chlorophyll biosynthesis pathway, we examined the expression of key genes in this pathway, including *protochlorophyllide oxidoreductase B* (*PORB*), *PORC*, *chlorophyllide a oxygenase* (*CAO*), and *geranylgeranyl reductase* (*GGRS*). Semi-quantitative RT-PCR analysis showed that the levels of *PORB*, *PORC*, *CAO*, and *GGRS* transcripts were greatly decreased in *emb1303-1* (Figure 8A), which likely contributes to the reduced chlorophyll level in the mutant. *CLA1* is directly involved in the carotenoid biosynthesis pathway, and its expression was also reduced in the mutant, resulting in the decreased levels of carotenoid.

We further chose nuclear- and chloroplast-encoded genes expressed at different stages of chloroplast development to characterize the plastid differentiation stages in *emb1303*. The transcript levels of *accD* [29, 30] and *rrn16S* [29], marker genes for plastid transcription and translation, respectively, remained the same in the mutant (Figure 8A). This indicates that plastid transcription and translation during the early phases of chloroplast development are not significantly affected by the mutation.

To gain further insight into the role of the *EMB1303* gene, we compared the genome-wide expression profile of *emb1303-1* seedlings with that of wild-type Col using the Affymetrix ATH1 Genechip (http://www.affymetrix.com/). A total of 1 682 genes were identified with more than threefold change in expression in *emb1303-1* as compared with the wild type, with 522 being upregulated and 1 160 downregulated (Supplementary information, Table S1). As expected, the *EMB1303* gene was more than 80-fold downregulated in *emb1303-1*. This Genechip result was validated by RT-PCR experiment. The expression of *PORB*, *PORC*, *CAO*, *GGRS*, and *CLA1* exhibited the same trend in both analyses (Figure 8A).

The differentially expressed genes can be grouped into three major functional categories: metabolism, growth and development, and cell regulation (Supplementary information, Table S1). Interestingly, many genes involved in photosynthesis, chloroplast development, and terpenoid or chlorophyll biosynthesis were drastically downregulated in *emb1303-1*. Most of them were nuclear-encoded genes, consisting of 14 genes encoding chlorophyll a/b-binding proteins, 19 genes encoding subunits of PSI or II, and 14 genes encoding proteins involved in chlorophyll and carotenoid biosynthesis (Supplementary information, Table S2). It is noteworthy that the expression of chloroplast-encoded genes, including *psaA*, *psaB*, *psbA*, *psbB*, *psbD*, *psbE*, *psbG*, *psbT*, *ndhG*, and *rbcL* were also reduced in *emb1303-1* (Supplementary information, Table S2). Collectively, these results indicate

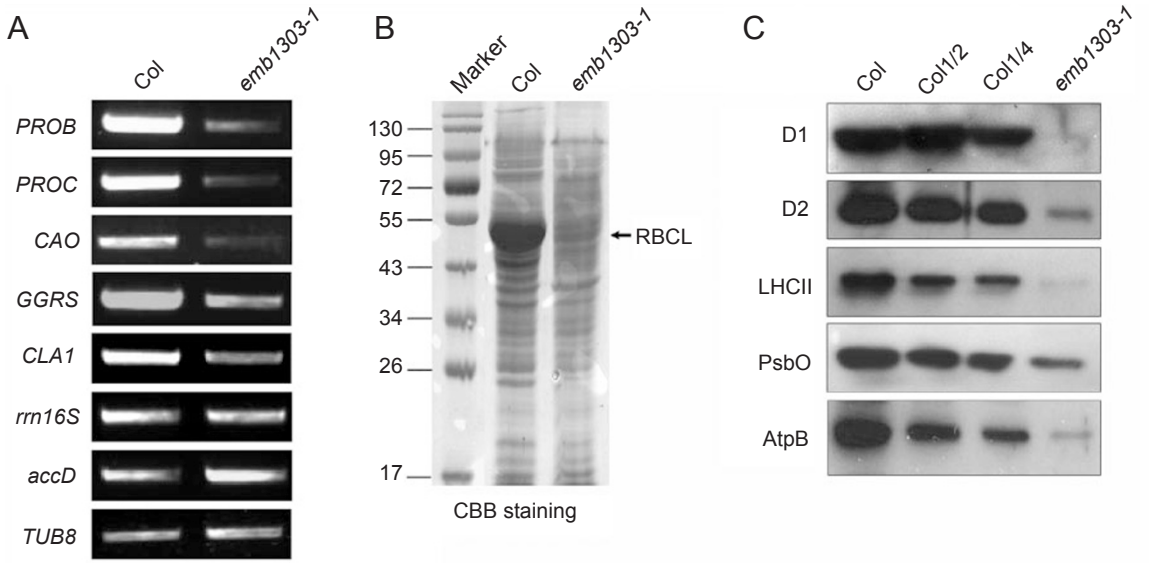

Figure 8 Gene expression and chloroplast protein expression in *emb1303-1* plants. **(A)** Expression of nuclear- and chloroplast-encoded genes. Total RNA prepared from 3-week-old seedlings of Col and *emb1303-1* grown on 1/2 MS media containing 2% sucrose was used for semi-quantitative RT-PCR. The *β-tubulin gene* (*TUB8*) was used as a quantitation control. **(B)** Coomasssie brilliant blue staining of total proteins. Total proteins were extracted from seedlings used in **(A)** and separated by SDS-PAGE. RBCL refers to the large subunit of Rubisco. **(C)** Immunoblot analysis of chloroplast proteins. Total proteins were analyzed by immunoblotting with antibodies against D1, D2, LHCII, PsbO, and AtpB proteins.

that EMB1303 is required for the expression of genes involved in photosynthesis and chloroplast development.

Immunoblot analysis of chloroplast proteins in emb1303-1

To further investigate chloroplast development in *emb1303-1*, we analyzed protein profile of *emb1303-1*. A significant reduction of the large subunit of Rubisco (RBCL) was observed by Coomassie brilliant blue staining (Figure 8B). Immunoblot analyses were also performed with antibodies raised against proteins involved in photosynthesis including D1 and D2 of PSII (encoded by *psbA* and *psbD*), the light-harvesting chlorophyll a/b-binding protein (LHCII), a 33-kD protein of the oxygen-evolving complex (PsbO), and the β subunit of the ATP synthase (AtpB). D1 and LHCII were barely detectable in *emb1303-1*, while D2, PsbO, and AtpB were dramatically reduced (Figure 8C). These results indicate that there are severe defects in the accumulation of photosynthetic protein complexes in *emb1303*.

Discussion

In this study, we identified a novel albino mutant *emb1303* and analyzed the role of the chloroplast-targeted EMB1303 protein in chloroplast development.

Loss of EMB1303 activity results in a complete arrest of plant growth and development and seedling lethality when grown in soil. Although *emb1303* mutants could develop through the vegetative stage and even produce inflorescences on the media with sucrose, they are infertile. This shows the necessity of sucrose as an energy source for the mutant growth, indicating that *EMB1303* is necessary for the photoautotropic growth of plants.

Though the biochemical activity of EMB1303 is unknown, several lines of evidence suggest that EMB1303 is essential for normal plant growth and chloroplast development. RT-PCR and promoter-reporter analyses have shown that *EMB1303* is expressed in almost all tissues and stages. EMB1303-GFP subcellular localization in both *N. benthamiana* leaves and *Arabidopsis* protoplasts verifies that EMB1303 is targeted to chloroplast, which was confirmed by immunoblot analysis. Ultrastructure analysis indicates that the plastids of *emb1303* are not fully developed and stacked thylakoid membranes are absent in the mutant. Thus, the functional EMB1303 protein is likely required for chloroplast development. Notably, the levels of chlorophyll and carotenoids are dramatically decreased in *emb1303*, which is consistent with the reduced expression of key genes for chlorophyll and carotenoids biosynthesis, including *PORB*, *PORC*, *CAO*, *GGRS*, and *CLA1*. Moreover, chloroplasts of *emb1303* are impaired at the early developmental stage, and the accumulation of chloroplast-encoded proteins such as D1 and D2 is significantly affected in *emb1303*. Consistent with the notion that the impaired chloroplast influences the expression of nuclear genes encoding plastid-localized proteins via retrograde signaling [31, 32], many nuclear genes that are involved in photosynthesis and chloroplast development are downregulated in *emb1303* (Supplementary information, Table S2). Alteration of expression of these genes could be responsible for the impaired photosynthetic ability and photoautotrophic growth of *emb1303*.

In addition to the defect in chloroplast, embryo development of *emb1303* is significantly slower than that of the wild type, indicating an important role of EMB1303 in embryogenesis. Our observation is consistent with previous studies showing that albino or pale-green mutants such as *edd1*, *slp*, and *dcl* with defective chloroplast development exhibit abnormal embryogenesis [6, 15, 17]. One possibility is that defective embryo development observed in *emb1303* is due to photosynthetic dysfunction caused by impairment of thylakoid membranes. It is also possible that the amount of biosynthetic products necessary for embryo development is not enough for the *emb1303* embryo to undergo a normal development rate. Further dissection of the biochemical nature of EMB1303 will shed more light on its function in chloroplast development and embryogenesis.

Materials and Methods

Plant material and growth conditions

Arabidopsis thaliana plants were grown at 22 ºC under a 16-h light/8-h dark photoperiod at 100 μmol m^{-2} s^{-1}, with 50-70% relative humidity. *Arabidopsis* seeds were either directly sown on soil or grown on Petri dishes containing half-strength MS basal salt mixture medium (Sigma) with 2% sucrose and 0.8% agar. *N. benthamiana* plants were cultivated in greenhouse under a 16-h-light/8-h-dark photoperiod with 50-60% relative humidity at 25 ºC.

Two lines with T-DNA insertions in *EMB1303*, *emb1303-1* (SALK_016097) and *emb1303-2* (CS16150), were obtained from ABRC. The T-DNA insertion sites were identified by sequencing PCR products amplified from the mutants with T-DNA primers and gene-specific primers EMB1303-1F and EMB1303-1R.

Plasmid construction and plant transformation

Probest High fidelity DNA polymerase (Takara) was used for the amplification reactions and constructs were verified by sequencing.

For the *pEMB1303::GUS* fusion, a 1.6-kb genomic fragment upstream of the *EMB1303* ATG start codon was amplified by PCR using EMB1303-p1F and EMB1303-p1R primers, and it was transcriptionally fused with the GUS reporter gene in the binary vector PZP212 [33].

To construct *p35S::EMB1303-GFP*, a 1.05-kb genomic fragment of *EMB1303* was amplified using the primers EMB1303-

2F and EMB1303-2R, and cloned into the *Sma*I and *Xba*I sites of either pUC-GFP or pGPTVII.GFP [34].

For the molecular complementation assay, a 5.2-kb *Pst*I-*Xba*I genomic fragment comprising the *EMB1303* promoter, the coding region, and the 3′-UTR region isolated from the BAC clone F14G9 from ABRC was cloned into the binary vector pCAMBIA1300 (CAMBIA, Canberra, Australia) to generate the *pEMB1303::EMB1303* construct.

Agrobacterium tumefaciens strain GV3101 [35] carrying different constructs was used to transform wild-type Col or heterozygous *emb1303* mutant plants via floral dip transformation [36]. *A. tumefaciens carrying p35S::EMB1303-GFP* or *p35S::GFP* plasmid was infiltrated into *N. benthamiana* leaves as described [34].

Quantitative RT-PCR

Total RNA was isolated from 3-week-old plants with TRI Reagents, followed by treatment with RNase-free DNase I (Promega, Madison, WI, USA) at 37 ºC for 1 h to degrade genomic DNA. Treated RNA samples (1 μg each) were used as templates for first-strand cDNA synthesis (Promega). The resulting cDNAs were then subjected to PCR amplification using gene-specific primers. The PCR-amplified samples were separated on 1% (w/v) agarose gels. Three RT-PCR reactions were repeated independently using *β-tubulin 8* (*TUB8*) as an internal control. Nucleotide sequences of gene-specific primers are available in Supplementary information, Table S3.

GUS assay

Histochemical detection of GUS activity was performed as previously described [33]. Tissues for GUS staining were incubated in staining solution (50 mM sodium phosphate, pH 7.0, 10 mM EDTA, 2 mM 5-bromo-4-chloro-3-indoyl glucuronide, 1 mM potassium ferricyanide, and 1 mM potassium ferrocyanide) at 37 ºC overnight. After incubation, stained tissues were cleared of chlorophyll in an ethanol series (20%, 40%, 60%, 80%, and 100%) and used for observation and photography.

Analysis of chlorophyll and carotenoids

Total chlorophylls and carotenoids were determined as described previously [37] with little modifications. Extracts were obtained from 21-day-old *Arabidopsis* seedlings grown on 1/2 MS medium. Fresh tissues were homogenized in 80% acetone. Spectrophotometric quantification was carried out in a Beckman DUR650 spectrophotometer. Pigment measurements were repeated in three independent experiments.

Protoplast preparations and chloroplast isolation

Protoplast preparations were performed as described [38]. Briefly, protoplasts were prepared 3 days after infiltration by incubating leaf strips in buffer (500 mM mannitol, 10 mM $CaCl_2$, 5 mM MES/KOH (pH 5.5), 3% cellulase, and 0.75% Macerozym). Intact chloroplasts were isolated as previously described [39] with modifications. Protoplasts were broken and centrifuged for 7 min at 1 000× g. The pellet was resuspended in buffer (0.45 M sorbitol, 50 mM Hepes-KOH pH 7.8, 2 mM EDTA, 0.1% BSA, 2.5 mM $MgCl_2$, and protease inhibitor cocktail), and then layered on a discontinuous 40%/80% Percoll gradient. After centrifugation for 15 min at 7 000× *g*, intact chloroplasts were isolated at the interface of the two layers, followed by two washes in buffer (0.33 M sorbitol, 50 mM Hepes-KOH pH 7.8, 2.5 mM $MgCl_2$, and protease inhibitor cocktail) with centrifugation for 5 min at 1 000× *g*.

Protein extraction and immunoblot analysis

Protein was isolated from tissues by pulverizing the tissue in ice-cold protein isolation buffer (60 mM Tris-HCl, pH 8.0, 50 mM NaCl, 10 mM EDTA, 30 mM β-mercaptoethanol, and 0.5 mM phenylmethanesulfonyl fluoride). Pulverized tissues were thoroughly mixed and cell debris was cleared by centrifugation at 12 000× *g* for 10 min at 4 ºC. Protein concentrations were determined according to the method described [40] with bovine serum albumin as standard.

Extracts were fractionated by SDS-PAGE on 10% (w/v) gel (30:0.8 (w/w) acrylamide:bis-acrylamide) using a minigel system (Bio-Rad Laboratories, Richmond, CA, USA). After electrophoresis, the separated proteins were visualized by Coomassie Brilliant Blue G-250, or transferred electrophoretically onto a PVDF nitrocellulose membrane (Bio-Rad). After blotting, blots were incubated with antibodies at a 1:3 000 dilution. Immunodetection was carried out using the secondary antibody (horseradish peroxidase IgG (H+L)) and Western Blotting Luminol Reagent (Santa Cruz, CA, USA).

Fluorescence microscopy

The autofluorescence (red) of chloroplasts and fluorescence of GFP in the transformed *N. benthamiana* leaves or protoplasts were imaged using a confocal laser scanning microscope (LSM510, Carl Zeiss, Oberkochen, Germany) at 2-4 days after infiltration.

To detect chlorophyll autofluorescence, leaf samples were examined by using a fluorescence microscope (Olympus Z61, Japan) with a long-pass 590-nm filter set.

Light and electron microscopy

To examine the development of the embryos, ovules from different developmental stages were treated with a clearing solution of chloral hydrate, water, and glycerol (8:2:1, v/v) for 12 h. The developing embryos were then analyzed under a Nomarski microscope (Leica DM 2500, Japan).

Sections of leaf tissue were prepared for electron microscope analysis observation as previously described [10] with minor modifications. Briefly, *Arabidopsis* leaf tissue was fixed with glutaraldehyde followed by osmium tetroxide and dehydrated in an ethanol series before being infiltrated with Spurr's resin (Dow Chemical Co., USA). Polymerization was conducted at 70 ºC for 8 h. Specimens were sliced to yield ultra-thin sections (LKB-8800, Sweden) and stained with uranyl acetate and alkaline lead citrate before being examined with a JEM-100S transmission electron microscope.

Microarray analysis

Affymetrix GeneChip ATH1 arrays representing ~24 000 *Arabidopsis* genes were used for the analysis of whole genome gene expression profile in wild-type Col and *emb1303-1* plants. Microarray experiments and data analysis were performed according to the manufacture's instruction (http://www.affymetrix.com/support/technical/manuals.affx). Briefly, total RNAs were extracted using the Plant RNA Prep Kit (Qiagen, Hilden, Germany) from 3-week-old seedlings of the mutant and the wild type grown on 1/2 MS medium containing 2% sucrose. In all, 5 μg of total RNA

was used to synthesize Cy3- and Cy5-labeled cDNA, which was then hybridized with the ATH1 oligonucleotide chips as instructed by the manufacturer (Affymetrix). The raw microarray data were analyzed using Microarray Suite 5.0 software (Affymetrix).

Acknowledgments

We thank Dr Lixin Zhang (Institute of Botany, Chinese Academy of Sciences) for providing antibodies of D1, D2, LHCII, and AtpB; and Arabidopsis Biological Research Center for T-DNA mutant seeds. We are grateful to Drs Jian Hua (Cornell University) and Hao Yu (National University of Singapore) for critically reviewing the manuscript. This work was supported by grants from National Natural Science Foundation of China (Nos. 30670181 and 30770202), the Ministry of Science and Technology of China (No. 2009CB119103), Program for New Century Excellent Talents in University (No. NCET-05-0124), and the Key Project of Chinese Ministry of Education (No. 106037).

References

1 Staehelin LA, Newcomb EH. Membrane structure and membranous organelles. In: Buchanan RB, Gruissem W, Jones RL, eds. *Biochemistry and Molecular Biology of Plants*. American Society of Plant Biology: Madison 2000:2-50.
2 Lopez-Juez E, Pyke KA. Plastids unleashed: their development and their integration in plant development. *Int J Dev Biol* 2005; **49**:557-577.
3 Taylor WC. Regulatory interactions between nuclear and plastid genomes. *Annu Rev Plant Physiol Plant Mol Biol* 1989; **40**:211-233.
4 Meurer J, Meierhoff K, Westhoff P. Isolation of high-chlorophyll-fluorescence mutants of *Arabidopsis thaliana* and their characterisation by spectroscopy, immunoblotting and northern hybridisation. *Planta* 1996; **198**:385-396.
5 Plucken H, Muller B, Grohmann D, Westhoff P, Eichacker LA. The HCF136 protein is essential for assembly of the photosystem II reaction center in *Arabidopsis thaliana*. *FEBS Lett* 2002; **532**:85-90.
6 Apuya NR, Yadegari R, Fischer RL, *et al*. The *Arabidopsis* embryo mutant schlepperless has a defect in the chaperonin-60α gene. *Plant Physiol* 2001; **126**:717-730.
7 Motohashi R, Nagata N, Ito T, *et al*. An essential role of a TatC homologue of a Δ pH- dependent protein transporter in thylakoid membrane formation during chloroplast development in *Arabidopsis thaliana*. *Proc Natl Acad Sci USA* 2001; **98**:10499-10504.
8 Sundberg E, Slagter JG, Fridborg I, *et al*. ALBINO3, an *Arabidopsis* nuclear gene essential for chloroplast differentiation, encodes a chloroplast protein that shows homology to proteins present in bacterial membranes and yeast mitochondria. *Plant Cell* 1997; **9**:717-730.
9 Klostermann E, Droste Gen Helling I, Carde JP, Schunemann D. The thylakoid membrane protein ALB3 associates with the cpSecY-translocase in *Arabidopsis thaliana*. *Biochem J* 2002; **368**:777-781.
10 Wang Y, Kollmann R. Vascular differentiation in the graft union of *in-vitro* grafts with different compatibility. Structural and functional aspects. *J Plant Physiol* 1996; **147**:521-533.
11 Hsieh MH, Chang CY, Hsu SJ, Chen JJ. Chloroplast localization of methylerythritol 4-phosphate pathway enzymes and regulation of mitochondrial genes in ispD and ispE albino mutants in *Arabidopsis*. *Plant Mol Biol* 2008; **66**:663-673.
12 Guevara-Garcia A, San Roman C, Arroyo A, *et al*. Characterization of the *Arabidopsis clb6* mutant illustrates the importance of posttranscriptional regulation of the methyl-D-erythritol 4-phosphate pathway. *Plant Cell* 2005; **17**:628-643.
13 Dong H, Deng Y, Mu J, *et al*. The *Arabidopsis Spontaneous Cell Death1* gene, encoding a zeta-carotene desaturase essential for carotenoid biosynthesis, is involved in chloroplast development, photoprotection and retrograde signalling. *Cell Res* 2007; **17**:458-470.
14 Qin G, Gu H, Ma L, *et al*. Disruption of phytoene desaturase gene results in albino and dwarf phenotypes in *Arabidopsis* by impairing chlorophyll, carotenoid, and gibberellin biosynthesis. *Cell Res* 2007; **17**:471-482.
15 Uwer U, Willmitzer L, Altmann T. Inactivation of a glycyl-tRNA synthetase leads to an arrest in plant embryo development. *Plant Cell* 1998; **10**:1277-1294.
16 Apuya NR, Yadegari R, Fischer RL, Harada JJ, Goldberg RB. *RASPBERRY3* gene encodes a novel protein important for embryo development. *Plant Physiol* 2002; **129**:691-705.
17 Bellaoui M, Keddie JS, Gruissem W. DCL is a plant-specific protein required for plastid ribosomal RNA processing and embryo development. *Plant Mol Biol* 2003; **53**:531-543.
18 Garcion C, Guilleminot J, Kroj T, *et al*. AKRP and EMB506 are two ankyrin repeat proteins essential for plastid differentiation and plant development in *Arabidopsis*. *Plant J* 2006; **48**:895-906.
19 Patel R, Hsu SC, Bedard J, Inoue K, Jarvis P. The Omp85-related chloroplast outer envelope protein, OEP80, is essential for viability in *Arabidopsis*. *Plant Physiol* 2008; **148**:235-245.
20 Kobayashi K, Suzuki M, Tang J, *et al*. LOVASTATIN INSENSITIVE 1, a novel pentatricopeptide repeat protein, is a potential regulatory factor of isoprenoid biosynthesis in *Arabidopsis*. *Plant Cell Physiol* 2007; **48**:322-331.
21 Yu B, Wakao S, Fan J, Benning C. Loss of plastidic lysophosphatidic acid acyltransferase causes embryo-lethality in *Arabidopsis*. *Plant Cell Physiol* 2004; **45**:503-510.
22 McElver J, Tzafrir I, Aux G, *et al*. Insertional mutagenesis of genes required for seed development in *Arabidopsis thaliana*. *Genetics* 2001; **159**:1751-1763.
23 Ifuku K, Yamamoto Y, Ono TA, Ishihara S, Sato F. PsbP protein, but not PsbQ protein, is essential for the regulation and stabilization of photosystem II in higher plants. *Plant Physiol* 2005; **139**:1175-1184.
24 Bang WY, Jeong IS, Kim DW, *et al*. Role of *Arabidopsis* CHL27 protein for photosynthesis, chloroplast development and gene expression profiling. *Plant Cell Physiol* 2008; **49**:1350-1363.
25 Emanuelsson O, Nielsen H, von Heijne G. ChloroP, a neural network-based method for predicting chloroplast transit peptides and their cleavage sites. *Protein Sci* 1999; **8**:978-984.
26 Oelmuller R. Photooxidative destruction of chloroplasts and its effect on nuclear gene expression and extraplastidic enzyme levels. *Photochem Photobiol* 1989; **49**:229-239.
27 Koch KE. Carbohydrate-modulated gene expression in plants. *Annu Rev Plant Physiol Plant Mol Biol* 1996; **47**:509-540.

28 Borisjuk L, Nguyen TH, Neuberger T, *et al*. Gradients of lipid storage, photosynthesis and plastid differentiation in developing soybean seeds. *New Phytol* 2005; **167**:761-776.
29 Gutierrez-Nava Mde L, Gillmor CS, Jimenez LF, Guevara-Garcia A, Leon P. CHLOROPLAST BIOGENESIS genes act cell and noncell autonomously in early chloroplast development. *Plant Physiol* 2004; **135**:471-482.
30 Hajdukiewicz PT, Allison LA, Maliga P. The two RNA polymerases encoded by the nuclear and the plastid compartments transcribe distinct groups of genes in tobacco plastids. *EMBO J* 1997; **16**:4041-4048.
31 Koussevitzky S, Nott A, Mockler TC, *et al*. Signals from chloroplasts converge to regulate nuclear gene expression. *Science* 2007; **316**:715-719.
32 Nott A, Jung HS, Koussevitzky S, Chory J. Plastid-to-nucleus retrograde signaling. *Annu Rev Plant Biol* 2006; 57:739-759.
33 Yang S, Yang H, Grisafi P, *et al*. The BON/CPN gene family represses cell death and promotes cell growth in *Arabidopsis*. *Plant J* 2006; **45**:166-179.
34 Walter M, Chaban C, Schutze K, *et al*. Visualization of protein interactions in living plant cells using bimolecular fluorescence complementation. *Plant J* 2004; **40**:428-438.
35 Koncz C, Schell J. The promoter of TL-DNA gene 5 controls the tissue-specific expression of chimaeric genes carried by a novel type of *Agrobacterium* binary vector. *Mol Gen Genet* 1986; **204**:383-396.
36 Clough SJ, Bent AF. Floral dip: a simplified method for *Agrobacterium*-mediated transformation of *Arabidopsis thaliana*. *Plant J* 1998; **16**:735-743.
37 Lichtenthaler HK, Wellburn AR. Determination of total carotenoids and chlorophylls a and b of leaf extracts in different solvents. *Biochem Soc Trans* 1983; **11**:591-592.
38 Yoo SD, Cho YH, Sheen J. *Arabidopsis* mesophyll protoplasts: a versatile cell system for transient gene expression analysis. *Nat Protoc* 2007; **2**:1565-1572.
39 Barneche F, Winter V, Crevecoeur M, Rochaix JD. ATAB2 is a novel factor in the signalling pathway of light-controlled synthesis of photosystem proteins. *EMBO J* 2006; **25**:5907-5918.
40 Bradford MM. A rapid and sensitive method for the quantitation of microgram quantities of protein utilizing the principle of protein-dye binding. *Anal Biochem* 1976; **72**:248-254.

(**Supplementary information** is linked to the online version of the paper on the *Cell Research* website.)